http://dx.doi.org/10.5012/bkcs.2013.34.1.33

Effects of the Number of Satellites on Surface Plasmon Coupling of Core-Satellite Nanoassemblies

Jun Hee Yoon and Sangwoon Yoon*

Department of Chemistry, Institute of Nanosensor and Biotechnology, Dankook University, Gyeonggi 448-701, Korea
**E-mail: sangwoon@dankook.ac.kr*
Received October 3, 2012, Accepted October 28, 2012

Key Words : Core-satellite nanoassembly, Surface plasmon coupling, Adsorption kinetics

Noble metal nanoparticles have attracted much attention due to their unique optical properties, represented by surface plasmon resonance (SPR).[1] The resonance frequency of the surface plasmon varies with the size, shape, material, and local environment of the nanoparticles.[1-3] Another appealing means to tune the optical response of the nanoparticle systems is assembling nanoparticles, instead of modifying individual nanoparticles.[4,5] Coupling of surface plasmons of nanoparticles in close proximity shifts the SPR band of the assembly from that of the individual nanoparticles. The shift naturally depends on the extent of the coupling, and thus on the detailed structure of assemblies such as interparticle distance, allowing for an infinitely fine control of the optical properties.[6,7] Therefore, assembling nanoparticles in a controlled fashion is of paramount importance.

Recently, we developed a novel method to prepare core-satellite nanoassemblies with well-defined and easily controllable structural parameters in a colloidal dispersion state.[8] Selective desorption of large gold nanoparticles (AuNPs) against small AuNPs from glass substrates by sonication led to the production of ultrapure nanoassemblies. The nanoassemblies consist of large core AuNPs decorated by small satellite AuNPs with a distance defined by self-assembled monolayers (SAMs) of alkanedithiol linkers. Different lengths of the alkanedithiol linkers allowed us to measure the surface plasmon couplings between the AuNP core and satellites as a function of the interparticle distances.

In complex nanoclusters, the surface plasmon coupling also depends on the number of nanoparticles that constitute the nanoclusters. For example, the surface plasmon coupling band continuously red-shifts as more nanoparticles are assembled in one direction.[9] This is intuitively understood as the red-shifting longitudinal surface plasmon mode supported by elongated nanostructures.

Contrary to linear assemblies, core-satellite nanoassemblies can be regarded as multiples of a size-asymmetric heterodimer consisting of a core and a satellite. In this simplified picture, the addition of satellites should not influence the surface plasmon coupling frequencies, although it will increase the intensity of the coupling. In this respect, it is intriguing to experimentally explore the surface plasmon coupling of the core-satellite nanoassemblies as a function of the number of satellites.

The new assembly method we developed enables facile control over the number of satellites in the nanoassembly.[8] The following process was used for the production of core-satellite nanoassemblies: (1) surface functionalization of glass substrates with amine, (2) adsorption of core AuNPs (50 ± 5 nm) on the glass substrate, (3) thiol-functionalization of the adsorbed core nanoparticles using 1,10-decanedithiol (DDT) SAMs, (4) adsorption of satellite AuNPs (13 ± 1 nm), and (5) selective desorption of the core-satellite nanoassemblies into ethanol by sonication.

The immersion time in step 4, allowed for the satellite AuNPs in solution to interact with the core AuNPs on the glass substrate, determines the number of satellites covering the core nanoparticles (Figure 1(a)). Transmission electron microscopy (TEM) images of more than 100 final core-satellite

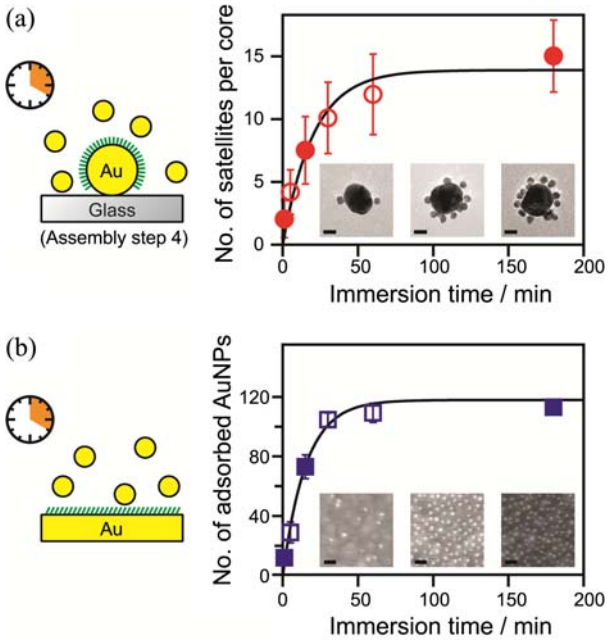

Figure 1. The number of AuNPs (13 nm) adsorbed on (a) DDT-functionalized core AuNPs (50 nm) and (b) DDT SAMs on Au substrate, as a function of the interaction time between the AuNPs and the surfaces. The solid lines indicate the best fit by exponential functions. The inset images are representative TEM and SEM images of the core-satellite nanoassemblies and AuNP-adsorbed Au substrates, respectively, acquired at the immersion time indicated by the filled symbols. The scale bars: (a) 20 nm, (b) 50 nm.

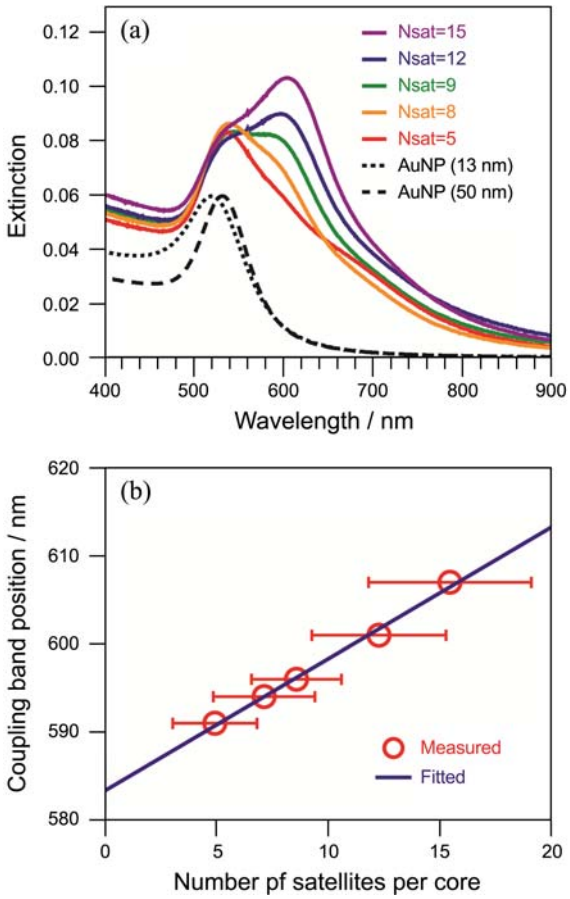

Figure 2. (a) UV-vis spectra of core-satellite AuNP assemblies with different number of satellites (N_{sat}). (b) The peak positions of the surface plasmon coupling bands as a function of the number of satellites. The solid line is the best linear fit.

nanoassemblies from each immersion time reveal that the number of satellites increases with immersion time (Figure 1(a)). The increase is best fitted to the exponential function, modeled by pseudo first-order adsorption kinetics where the satellite AuNPs in excess (4 nM) react with the limited number of adsorption sites on the surfaces of core AuNPs (5 pM) on the glass substrate.[10,11] From the fitting, we obtained the apparent rate constant, $(5.0 \pm 1.2) \times 10^{-2}$ min^{-1}. The error bars are one standard deviation, based on three separate experiments. The fitting curve reaches the asymptotic value, 14 ± 1, suggesting that the electrostatic repulsion among the citrate-capped satellite AuNPs allows only a limited number of the satellites to adsorb onto the core surfaces.

The adsorption kinetics is governed by the interaction between the thiol functional groups of the core AuNPs and citrate-capped satellite AuNPs. The nature of the adsorption was further tested by comparison with the adsorption of citrate-capped AuNPs on planar SAMs of DDT on gold substrates. The number of adsorbed AuNPs on planar SAMs, measured by scanning electron microscopy (SEM), follows a similar exponential rise with the immersion time (Figure 1(b)), yielding the comparable rate constant (6.5×10^{-2} min^{-1}).

Using these sets of ultrapure core-satellite nanoassemblies with controlled number of satellites, we measured the surface plasmon couplings. UV-vis spectra in Figure 2(a) show that the surface plasmon coupling bands are red-shifted from the SPR bands of the individual core and satellite AuNPs.[8] Additionally, the surface plasmon coupling band progressively intensifies and red-shifts as the number of satellites increases. Plotting the surface plasmon coupling wavelengths as a function of the number of satellites in Figure 2(b) suggests that the spectral response linearly red-shifts by 1.7 ± 0.2 nm per satellite.

The observed linear red-shift of the surface plasmon coupling with the increasing number of satellites is consistent with the theoretical studies by Lee and coworkers.[12] Using generalized multiparticle Mie (GMM) theory, they predicted an approximately 1 nm red-shift per satellite for a 100 nm core –20 nm satellite assembly system.

The continuing red-shift of the surface plasmon coupling band with the addition of satellites clearly suggests that the core-satellites cannot be treated simply as multiples of dimers. Rather, the surface plasmons of all constituting nanoparticles should be considered collectively. Adopting the surface plasmon hybridization model,[4] we believe that the addition of the satellites to the assembly causes more surface plasmon modes to be mixed in the hybridized surface plasmon modes, resulting in lowering the energy of the mode.

In summary, the controlled assembly of the core-satellite nanostructures allowed us to measure the surface plasmon coupling of the nanoassemblies with different number of satellites. The surface plasmon coupling band linearly red-shifts as the number of satellites increases. This work demonstrates that assembly of nanoparticles is a great way to tune the optical properties of the system in a wide range of wavelengths.

Acknowledgments. This work was supported by the Dankook University Research Fund (2010).

References

1. Kelly, K. L.; Coronado, E.; Zhao, L. L.; Schatz, G. C. *J. Phys. Chem. B* **2003**, *107*, 668.
2. Lal, S.; Link, S.; Halas, N. J. *Nat. Photonics* **2007**, *1*, 641.
3. Jain, P. K.; Lee, K. S.; El-Sayed, I. H.; El-Sayed, M. A. *J. Phys. Chem. B* **2006**, *110*, 7238.
4. Prodan, E.; Radloff, C.; Halas, N. J.; Nordlander, P. *Science* **2003**, *302*, 419.
5. Sheikholeslami, S.; Jun, Y.-W.; Jain, P. K.; Alivisatos, A. P. *Nano Lett.* **2010**, *10*, 2655.
6. Jain, P. K.; Huang, W.; El-Sayed, M. A. *Nano Lett.* **2007**, *7*, 2080.
7. Busson, M. P.; Rolly, B.; Stout, B.; Bonod, N.; Larquet, E.; Polman, A.; Bidault, S. *Nano Lett.* **2011**, *11*, 5060.
8. Yoon, J. H.; Lim, J.; Yoon, S. *ACS Nano* **2012**, *6*, 7199.
9. Zhong, Z.; Patskovskyy, S.; Bouvrette, P.; Luong, J. H. T.; Gedanken, A. *J. Phys. Chem. B* **2004**, *108*, 4046.
10. Park, J. J.; De Paoli Lacerda, S. H.; Stanley, S. K.; Vogel, B. M.; Kim, S.; Douglas, J. F.; Raghavan, D.; Karim, A. *Langmuir* **2009**, *25*, 443.
11. Rouhana, L. L.; Moussallem, M. D.; Schlenoff, J. B. *J. Am. Chem. Soc.* **2011**, *133*, 16080.
12. Ross, B. M.; Waldeisen, J. R.; Wang, T.; Lee, L. P. *Appl. Phys. Lett.* **2009**, *95*, 193112.